

A Theoretical and Numerical Evaluation of Stope Structural Parameters in Open Stopping and Subsequent Backfill

Lin Chen^{1*}, Qingling Liu¹, Wendong Li², Shaohui Tang³

¹Fuzhou University, Zijin School of Geology and Mining, Wulongjiang Road 2, Fuzhou 350108, China

*Corresponding Author E-mail: 2689794792[at]qq.com

²SERBIA ZIJIN COPPER DOO, DJORDJA VAJFE RTA29, Bor 19210, Serbia

³Zijin Mining Group Co., Ltd., Xiamen 361016, China

Abstract: *Open stopping and subsequent backfill is a mining method with high requirements for rock mechanical conditions and ore recovery. To optimize stope structural parameters in Jama copper mine, Serbia, A theoretical calculation and numerical simulation is carried out. Under the condition of keeping constant stope length and height, the reasonable range of structural parameters is obtained through the theoretical calculation of safe span. Further, FLAC^{3D} is used to simulate the stope stability under four schemes, and the displacement, plastic zone distribution, principal stress change and safety factor value are used as the criteria. The results show that when the stope structural parameters are 60 m in length, 18 m in room width, 15 m in pillar width and 40 m in height, there is no through failure in the whole mining process. When simulating the mining of the stope at -210 mL, safe and efficient mining is realized with the stable mined-out areas at upper stage. This study provides theoretical basis and technical reference for the sustainable development of BR ore body in Jama mine.*

Keywords: Open stopping and subsequent backfill, Safe span, Numerical simulation, Structural parameter optimization

1. Introduction

Open stopping and subsequent backfill is widely used in metal mines worldwide since its advantages of high mining and backfill efficiency, safe operation and low loss and dilution rate. With the gradual advancement of mining to the deep, it has irreplaceable advantages in ground pressure control, stope stability, operation safety and surface collapse control [1]. Moreover, Open stopping and subsequent backfill is a coordinating combination of backfill method and open stope method, and gradually forms the process characteristics of "high stage, large panel and mechanization". While inheriting the advantages of backfill method, it also has the advantages of high production efficiency, high mining intensity and safe working environment. It is a backfill mining method with highest production efficiency at present, representing the development direction of large-scale, high-efficiency and green mining [2].

It is of great theoretical significance to reasonably determine the structural parameters such as stope room span and roof thickness of open stopping and subsequent backfill. The optimization of stope structural parameters mainly includes theoretical calculation method [3-7], numerical simulation method [8-13], neural network method [14-15], etc. The existing study provides a more effective means for the optimization of stope structural parameters. Liu et al [16] used numerical simulation to analyze the stability of surrounding rock in order to improve mining rate and control roof stability. The results show that the stability of roof can be guaranteed by adopting stope structural parameters with room height of 16 m, room width of 6 m, roof cutting height of 4 m and floor mining height of 12 m. Wei et al [17] determined the stope parameters of the sublevel subsequent backfill stage of Tieshizishan mine according to the similar material

simulation, displacement monitoring and internal stress monitoring. T. Mall et al [18] simulated the stress change of ore pillar in four different stages in Bayındır lead-zinc mine, and proposed a designed stopping parameters with the safe deformation range. The above research cases of stope structure parameter provide important is valuable for safe and efficient production of mines.

Jama copper mine is an underground mine in production in Bor, Serbia. The main BR ore body is located in the northwest of Jama copper deposit, with an overall strike of NW-SE and a dip angle of 45 ~ 55°. The strike of the ore body is about 1450 m long and 360 m wide, extending about 1400 m vertically, and the occurrence elevation is 92~934 m. It is an inclined and extremely thick porphyry copper ore body. In this study, the safe and reasonable stope span of open stope method is firstly obtained by calculation of ultimate allowable span. Secondly, under the conditions of constant height and length at -150 mL, four schemes of variable room and pillar configurations at -210 mL are designed, and the stability of stope and mined-out areas in two stages of mining is simulated by FLAC^{3D}. Finally, combined with the theoretical calculation and numerical simulation results, the optimal stope structural parameters incorporating safety and economic factors in open stopping and subsequent backfill at Jama copper mine are determined.

2. Mine overview

2.1 Mining technical conditions

BR ore body in Jama mine is an inclined and extremely thick porphyry copper ore body. The joints and fissures of the ore body are generally developed, most of which are layered joints and mainly shear joints, and there are few tensile joints.

The joint spacing is 25~50 cm. The RQD value of rock quality index is 73.46%~82.02%, with an average of 77.31%, and the uniaxial compressive strength is 76.26 MPa. The main lithology is kaolinized andesite and silicified andesite. The rock has relatively low strength, high joint density and high water content. The hanging wall andesite has a RQD value of 72~80%, a uniaxial compressive strength of 60~110 MPa. The footwall is conglomerate and structural breccia existing in Bor fault, whose RQD value is 75~92% and the uniaxial compressive strength is 50 ~ 70 MPa.

2.2 Mining methods

At present, stopes at -150mL and above has basically completed mining, and -210 mL is under developing. The strike length of the ore body at -210 mL is about 660 m, the thickness of the ore body is 40~240 m, and the inclination angle is 45~55°. To ensure safety, -170 m~-150 m is designed as reserved roof, that is, the roof thickness is 20 m. The -210 m ore body is mined by open stoping and backfill with large-diameter and deep hole. The stope is arranged perpendicular to the direction of ore body, and the room and pillar are arranged at regular intervals. The mining sequence is mining one after another. The schematic diagram of this mining method is shown as follows:

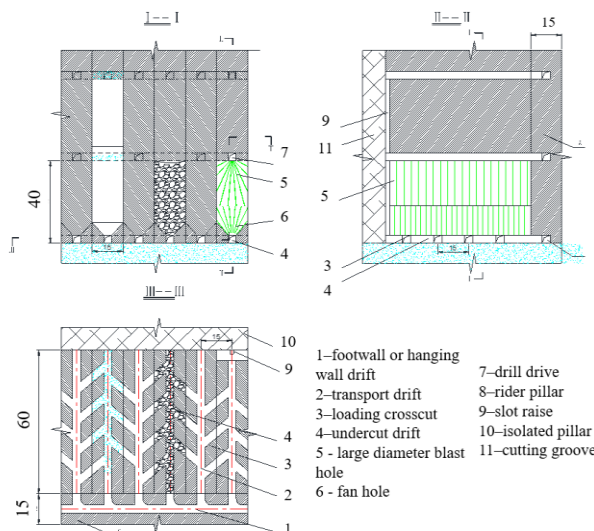


Figure 1: Schematic diagram of open stoping and backfill

3. Theoretical calculation of structural parameters

Stope span is an important factor in stope structural parameters. If the span is too large, it is easy to lead to bending failure and shear failure, resulting in roof fall accident. A reasonable room span is more reliable with numerical simulation after theoretical calculation. The thickness span ratio theory, load transfer line theory, simply supported beam theory and unsupported span are used to analyze the reasonable room span.

3.1 Thickness span ratio

According to the theory and calculation of thickness span ratio, if the ratio of roof thickness to room span is less than 0.5, it is considered that the roof is safe and stable. Considering the safety factor n , the relationship between

room span and roof thickness under different safety conditions can be obtained. The calculation formula is shown in Formula (1). According to the Formula (1), the room span is also a single factor function of the roof thickness. When the roof thickness is between 4~22 m, the corresponding limit span of the room is shown in Figure 2.

$$k \leq \frac{h}{0.5n} \quad \#(1)$$

where h is roof thickness, k is ultimate span of room, n is safety factor, taken as 1.3.

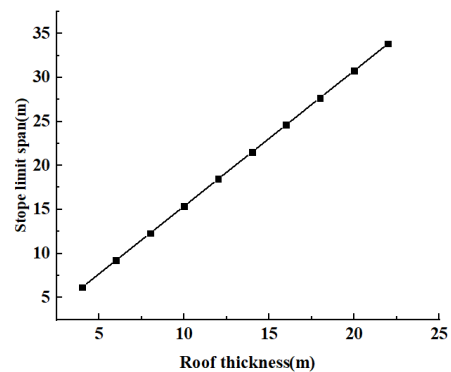


Figure 2: Relationship between ultimate room span and roof thickness

Figure 2 shows that the stope span of is also linearly proportional to the roof thickness. When the roof thickness is between 4 and 22 m, the ultimate room span is between 6.2 and 33.8 m.

3.2 Load transfer line theory

Assumes that the load is transmitted downward from the center of the roof at a diffusion angle of 30°~35° with the vertical line. When this transmission line is located outside the interstage of the roof and the side slope of the mined-out areas, it is considered that the side slope of the mined-out areas directly supports the external load and rock self-weight on the roof and the roof is safe. In this case, the calculation formula of the relationship between the safe roof thickness and the room span is:

$$L \leq 2htan\alpha \quad \#(2)$$

where L is room span, H is roof thickness, α is The included angle between the load transfer line and the vertical line in the roof center, taken as 32°.

According to the theoretical calculation formula of "load transfer interstage line", it can be seen that there is a positive correlation between the ultimate room span and the roof thickness. When the roof thickness is between 4~22 m, the corresponding ultimate room span is shown in Figure 3.

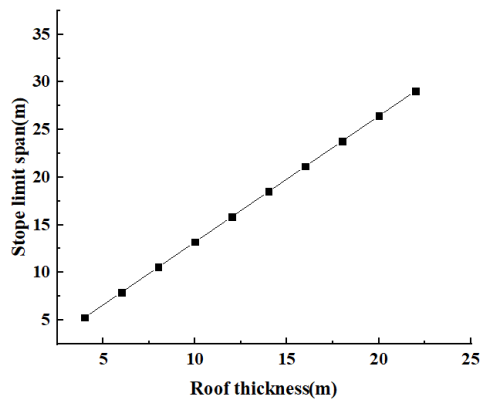


Figure 3: Relationship between limit room span and roof thickness obtained from "load transfer interstage line theory"

As can be seen from Figure 3, the room span is also linearly proportional to the roof thickness. When the roof thickness is 4~22 m, the limit span of the room is between 5.3~29.1 m. (0.14").

3.3 Simply supported beam theory

According to the simply supported beam theory of material mechanics, and considering the influence of rock beam self-weight and upper load on rock beam, the ultimate room span is calculated. In the stability analysis, the tensile stress in the roof rock is mainly considered, and according to the theory of material mechanics, the position where the maximum tensile stress is generated is on the lower surface of the middle of the beam. The mechanical model of rectangular simply supported beam is established, as shown in Figure 4.

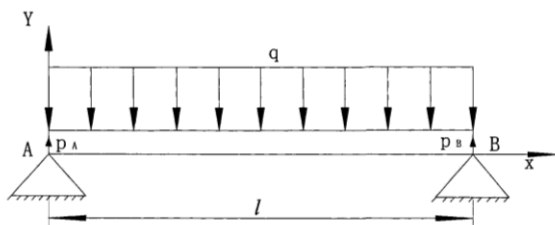


Figure 4: Mechanical model of simply supported beam in material mechanics

Assumes q is the load of the overlying strata on the roof, and the unit weight of the roof strata is γ , the width of the beam is l , the thickness is h , the span is z , and the support reaction force at both ends of the rock beam is p , then

$$p = \frac{ql}{2} + \frac{\gamma hl}{2} \quad \#(3)$$

Taking the left end point as the origin, calculate the bending moment M of the left half load of the beam on the cross stage in the middle of the beam, and the formula is as follows:

$$M = \frac{pl}{2} - \int_0^{\frac{l}{2}} \gamma h \left(\frac{l}{2} - x\right) dx - \int_0^{\frac{l}{2}} q \left(\frac{l}{2} - x\right) dx \quad \#(4)$$

Substitute equation (3) into equation (4) and integrate to get the next formula:

$$M = \frac{ql^2}{8} + \frac{\gamma hl^2}{8} \quad \#(5)$$

For the convenience of analysis, if the width of rectangular stage beam is taken as 1, the bending stage coefficient W_z of rectangular stage is:

$$W_z = \frac{bh^2}{6} \quad \#(6)$$

Maximum bending normal stress of beam σ_{\max} is

$$\sigma_{\max} = \frac{M}{W_z} \quad \#(7)$$

Substitute formula (5) and formula (6) into formula (7) to obtain the next formula:

$$\sigma_{\max} = \frac{3ql^2 + 3\gamma hl^2}{4h^2} \quad \#(8)$$

where q is uniformly distributed load of overburden, l is beam span, γ is unit weight of open roof rock stratum, h is beam thickness. The uniformly distributed load q of the overlying strata is obtained by Terzaghi formula^[19] and substituted into formula (8)

$$\sigma_{\max} = \frac{1.5\gamma_1 Hl^2 + 3\gamma_2 hl^2}{4h^2} \quad \#(9)$$

where γ_1 is average bulk density of the overlying rock mass, l is open stope span, λ is average lateral pressure coefficient of the overlying rock mass, ψ is average internal friction angle of the overlying rock mass, H is open stope depth, h is roof thickness, γ_2 is bulk density of the roof rock mass.

According to the calculation, the span of the room increases linearly with the increase of roof thickness. When the roof thickness is 4~22 m, the corresponding ultimate room span is 4.4~23.6 m. The roof thickness of BR ore body at -210 mL is reserved for 20 m, and therefore the corresponding room span is 21.5 m.

3.4 Maximum unsupported span

The relationship between the maximum unsupported span of underground excavation and Q value and excavation support ratio (ESR) is as follows:

$$\text{SPAN} = 2 \times (\text{ESR}) \times Q^{0.4} \quad \#(10)$$

where SPAN is span diameter or width of excavation body, ESR is support ratio of excavation body, Q is the classification index of Q system classification method.

The support ratio of the excavation is related to its usage and allowable instability. According to the recommended value of ESR proposed by Barton^[20] in 1976, when the mine roadway is used as a permanent project of the mine, $\text{ESR} = 1.6$. When the old mined-out areas and roadway are only used as a temporary channel of the mine, $\text{ESR} = 3.0 \sim 5.0$. According to Jama engineering geological survey, the Q value of ore and

rock is 17.18. The stope span can be calculated through formula (10). Since the mined-out areas is usually treated as a temporary channel, the maximum unsupported span of ore and rock can be calculated to be 18.72~31.20 m.

3.5 Theoretical evaluation

Under the condition of a constant roof thickness, the theoretical calculation value of the thickness span ratio is highest, and the theoretical calculation value of the simply supported beam in elasticity is lowest. When the roof thickness is 20 m, the ultimate room span calculated by the four theories is 18.72~21.5 m. From the perspective of stope safety, the minimum ultimate room span is taken as 18 m. Considering the loss rate, the pillar width should be less than 18 m. A batch of numerical simulation is carried out to further evaluate the reasonable stope structural parameters.

4. Numerical Simulation of structural parameters

4.1 Numerical simulation method

The numerical simulation object of stope stability is located at -210 mL, whose numerical model is 162° southeast along the strike of the ore body, as shown in Figure. 5 and 6. Based on the stope length of 60 m and mining height of 40 m in the mined -150 mL, the stope room length and height in the -210 mL are consistent with those in the previous stage. At present, the structural parameters of -150 mL stope are scheme 1, taking this as the control group, four reasonable schemes are formulated for analysis and comparison. The specific simulation scheme is shown in table 1. The simulation scheme considers the failure response process of different stope widths in one step during mining.

According to the current mining situation, the -150 mL is established, with 492 m long ore body along the strike, 12 m width ore room and 40 m mining height, number of 21 ore rooms are mined in one step. In the -210 mL, the ore body is 612 m long along the strike and the mining height is 40 m. The altitude range of the model is +0~-320 m and the length is 812 m. Based on the established analysis model, the stability of single stope, multi stope and panel pillar in Jama mine is studied from the aspects of stress field, displacement field, plastic zone and safety factor with Flac^{3D}.

Table 1: Margin specifications

Scheme	Room width /m	Pillar width h /m	Height/ m	Length/ m	Number of grids (10 ³)
1	12	12	40	60	78.90
2	15	15	40	60	79.50
3	16.5	15	40	60	78.24
4	18	15	40	60	80.10

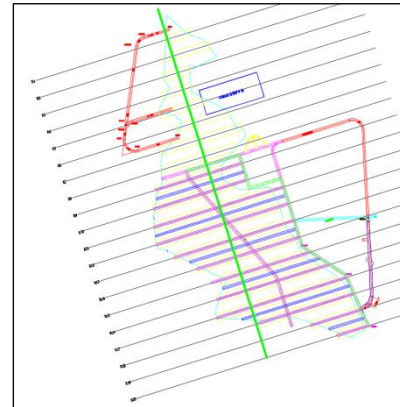


Figure 5: A plan view of BR ore body at -210 mL

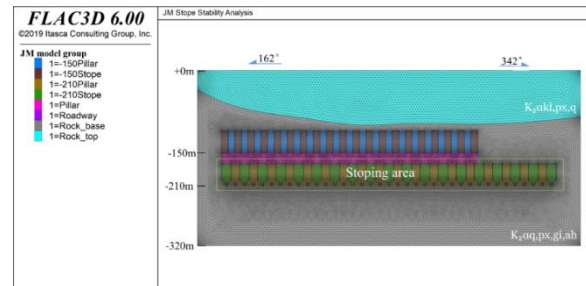


Figure 6: Schematic diagram of numerical simulation model of stope stability

The surface elevation of Jama mine is +398 m. When the buried depth of the ore body is -320 m (i.e. the bottom of the model), the vertical self-weight stress of the overlying strata is 19.0 MPa. The calculated initial in-situ stress of the stope along the strike is 15.2 MPa and the initial in-situ stress along the vertical strike is 22.8 MPa. Rigid constraints are adopted for the bottom perimeter of the analysis model, displacement constraints are adopted for the side along the strike direction, displacement constraints are adopted for the side perpendicular to the strike, and flexible constraints are adopted for the top of the model. The initial stress field is inverted through the elastic constitutive model. The Mohr-Coulomb ideal elastic-plastic model is used for the subsequent mining process analysis, and the empty element model is used for the excavation process. The physical and mechanical parameters of medium are mainly the mechanical parameters of ore body and surrounding rock. Mechanical parameters of ore body, surrounding rock and backfill are shown in Table 2.

Table 2: Physical and mechanical parameters of analytical medium

Type	Ore body	Hanging wall	Footwall
Strength of rock /MPa	76.26	71.92	49.27
Strength of rock mass/MPa	19.06	17.98	12.32
Tensile strength /MPa	0.66	0.64	0.3
Elastic modulus /GPa	36.83	35.76	29.6
Cohesion /MPa	7.147	6.25	4.62
Internal friction angle /°	45.81	42.45	35.8
Poisson's ratio	0.26	0.3	0.31

4.2 Results of numerical simulation

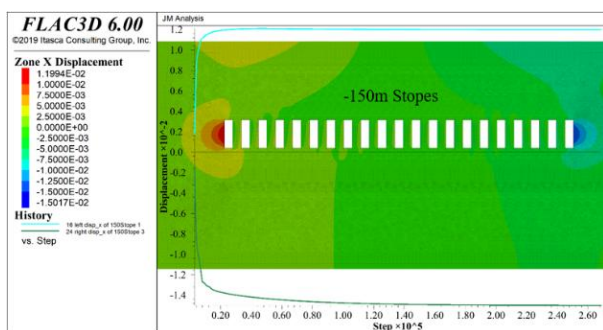
The simulation results are analyzed by taking the structural parameters of the stope room with a width of 15 m and a

height of 100 m as an example. Step 1 represents the stope in the mining at -150 mL, and Step 2 represents the stope in the mining at -210 mL. In the process of simulation calculation, Step 1 is firstly carried out, and then Step 2 is proceeded. The distribution law of stress field, plastic zone and safety factor in the mining process is analyzed, and the simulation results of each scheme are finally summarized, and the optimal stope structural parameters are proposed.

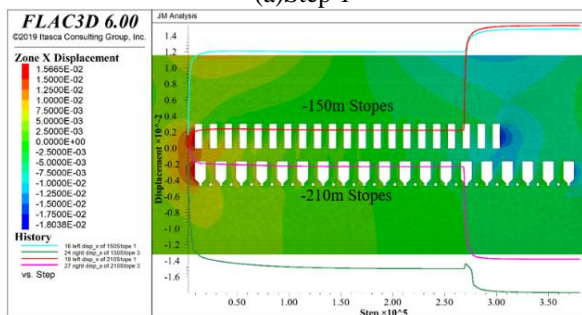
4.2.1 Displacement field

(1) Horizontal displacement monitoring (along the ore body trend)

As shown in Figure 7 (a), when Step 1 is completed, the left side of the leftmost stope (south end) and the right side of the rightmost stope (north end), produce the maximum horizontal displacement at -150 mL, and the horizontal displacement value is 11.9~15.0 mm. The horizontal displacement at the south and north ends of -150 mL continues to increase with the recovery of -210 m stope, with the increase value of 2.0~3.0 mm to 14.0~17.9 m (Figure 7 (b)). Therefore, in the case of stage pillar, the mining of -210 m stope has little effect on the horizontal displacement of -150 m stope. After the completion of Step 2 mining, the left side of the leftmost stope (south end) and the right side of the rightmost stope (north end), produce the maximum horizontal displacement at -210 mL. The horizontal displacement value is 15.4 mm, and the horizontal displacement values of other stopes are lower than this value.



(a)Step 1



(b)Step 2

Figure 7: Horizontal displacement curve of left and right sides of stope

(2) Vertical displacement (gravity direction)

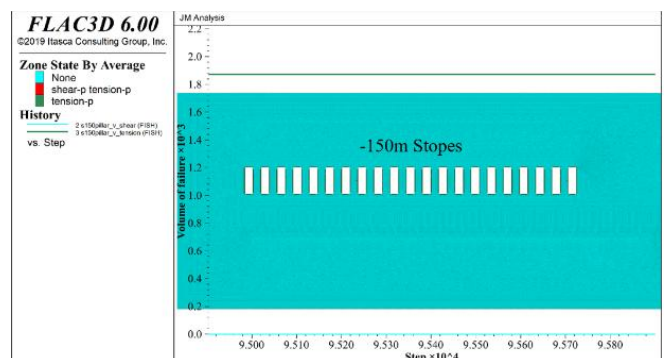
As shown in Figure 8 (a), after Step 1 mining, the maximum vertical displacement of the roof and floor at -150 mL, and the displacement of the roof of the stope is greater than that of the floor. The displacement value of the roof and floor of

the middle stope is 20.2 mm and 6.0 mm respectively. As shown in Figure 8 (b), with the stope of -210 mL, the vertical displacement direction of the bottom plate of the middle stope in -150 mL changes from upward to downward, showing settlement, from 5.5 mm (upward) to 17.5 mm (downward). At -150 mL, the vertical displacement of the middle stope roof continues to increase, and the displacement value increases from 20.5 mm (downward) to 42.6 mm (downward), with a change value of 22.1 mm. After mining of Step 2, the floor displacement of the middle stope at -210 mL is slight, with the displacement value of 5.0 mm (upward) and the roof displacement value of 24.5 mm.

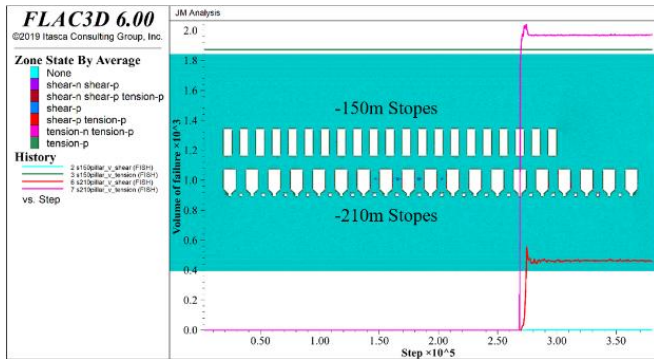
4.2.2 Distribution of plastic zone

After mining of Step 1, the failure form of pillars in each stope at -150 mL is mainly tensile failure, and the total volume of tensile failure body is 1871.8m³/m (Figure 9 (a)). According to the mining status of -150 mL (number of 21 ore rooms and 20 pillars), the tensile failure volume of pillars in each stope is 93.59 m³/m, accounting for 19.5% of the total mining volume of stope. The main cause of tensile failure lies in the large deformation of stope roof and floor and two sides. From the perspective of stress transfer and release in panel stope, the local tensile failure caused by Step 1 will be conducive to the release of stress and the recovery of the room in the next stage. Due to the existence of pillar at -210 mL, the mining at -210 mL does not affect the stability of pillar at -150 mL, and the tensile and shear failure volume of pillar at -150 mL does not change with the mining at -210 mL, which remains basically unchanged.

Figure 9 (b) shows the bottom drawing roadway, bottom structure and stope pillar sidewall produce local tensile failure. The total volume of tensile failure is 2049.0 m³/m (unit stope length). According to the preliminary design of -210 mL mining (number of 19 ore rooms and 18 pillars), the tensile failure volume of each stope pillar is 113.83m³/m, accounting for 16.7% of the total stope mining. The pillars of the four stopes in the middle have local shear failure, with a small failure volume of 437.2 m³/m (unit stope length), and there is no through failure. The research shows that the stope room width is 18 m and the pillar width is 15 m (i.e. scheme 4), which tends to be horizontal deformation and produce tensile failure. The shear failure of stope pillar will expand outward from the center of stope pillar.

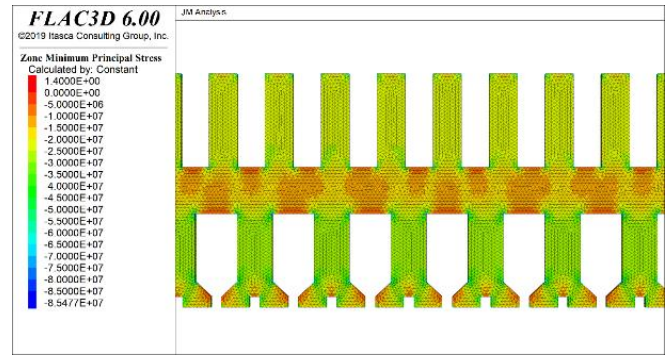


(a)Step 1

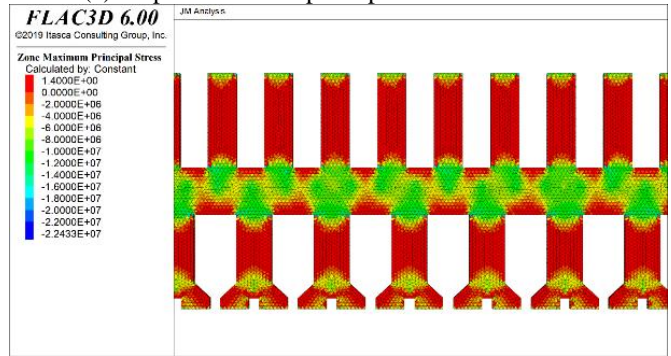


(b) Step 2

Figure 9: Failure volume curve of stope pillar



(c) Step 2 Minimum principal stress distribution

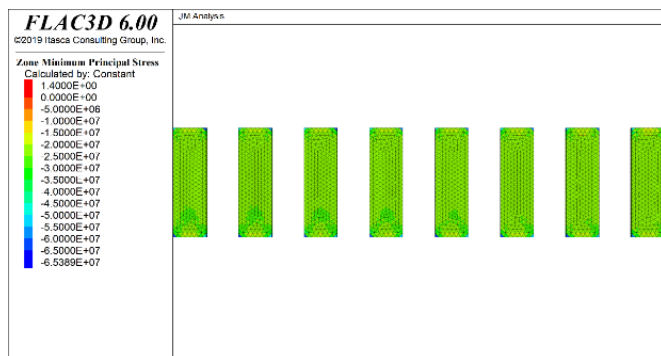


(d) Step 2 Maximum principal stress distribution

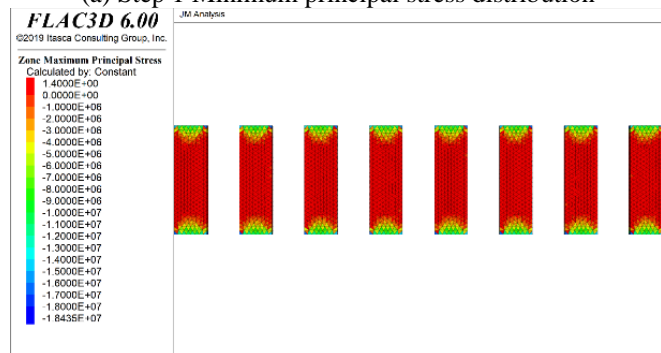
Figure 10: Distribution of principal stress during mining

4.2.3 Principal stress

After mining at -150 mL, the four corner boundaries of the mining pillar are prone to local stress concentration, and the stope pillar is generally under pressure (Figure 10 (a&b)). The average minimum principal stress of stope pillar is $\sigma_1=27.36$ MPa (pressure), the corresponding maximum principal stress is $\sigma_3=0.068$ MPa (tension). Figure 10 (c&d) shows that the stope pillar is still under overall pressure after mining at -210 mL. The average minimum principal stress of stope pillar at -150mL is basically consistent with Step 1, which is $\sigma_1=27.51$ MPa (pressure), the maximum principal stress is $\sigma_3=0.067$ MPa (tension). Average minimum principal stress of stope pillar at -210 mL is $\sigma_1=32.68$ MPa (pressure), corresponding average maximum principal stress $\sigma_3=0.12$ MPa (tension).



(a) Step 1 Minimum principal stress distribution



(b) Step 1 Maximum principal stress distribution

4.2.4 Safety factor

The safety factor of stope excavation is evaluated by strength stress ratio index. Strength stress ratio (SSR) refers to the ratio of the yield strength of rock mass to the actual stress, which describes the proximity between the current stress state of the unit and the failure stress state. Minimum stress of assumed element σ_1 and the maximum stress is σ_3 . The stress Mohr's circle in the current state is shown in Figure 11. The safety rate is the ratio of the ultimate stress state determined by Mohr-Coulomb strength criterion to the actual stress state. When the safety rate is 1, it is in a critical state. The greater the safety rate, the better the stability of surrounding rock. If the maximum principal stress is maintained σ_3 unchanged, the minimum principal stress corresponding to the new critical Mohr's circle can be obtained σ_1' . The strength stress ratio is defined as:

$$SSR = \frac{\sigma_1' - \sigma_3}{\sigma_1 - \sigma_3} \quad \#(10)$$

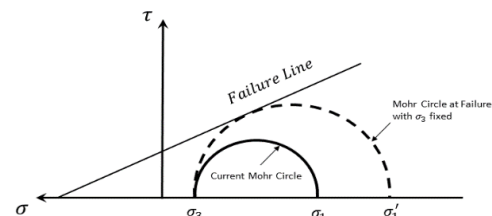
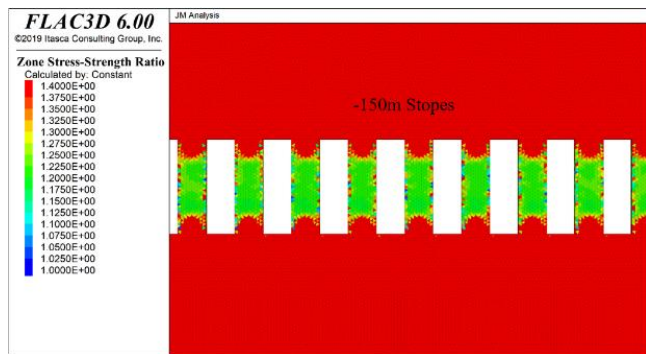


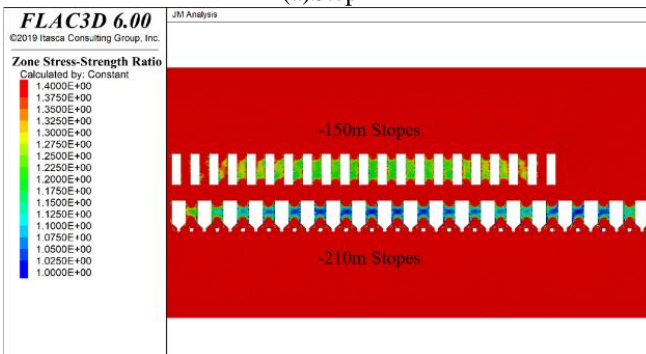
Figure 11: Mohr's circle diagram of element stress state

According to the definition of strength stress ratio, Figure 12 (a) shows the strength stress ratio distribution of shear failure in the range of 1.0~1.4 after mining of Step 1. The stress intensity ratio of stope pillar is mostly in a safe state, and only a few grid elements have shear failure.

After Step 2, the safety factor of two areas of stope pillar at -210 mL is close to 1.0, one is the central stope pillar, and the other is the mining pillar close to the northern boundary of the stope in the previous stage (Figure. 12 (b)). The distribution diagram of strength stress ratio shows that the stress redistribution caused by stope mining will reduce the safety factor of stope pillar, and the safety factor distribution is consistent with the distribution of model plastic zone. The bottom structure of the trench and the two sides of the ore drawing roadway are prone to shear failure and have a penetration trend, and the shear trace of the two sides presents a concave radian. The simulation results show that the bolt or anchor cable should be used to support the bottom structure. When the two sides of the trench bottom structure are supported, the bolt or anchor cable should deflect downward and penetrate the shear circle.



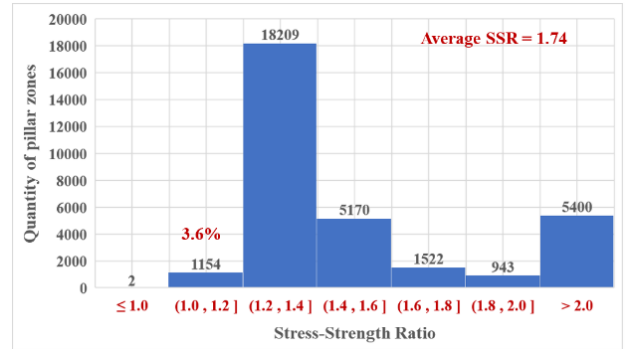
(a)Step 1



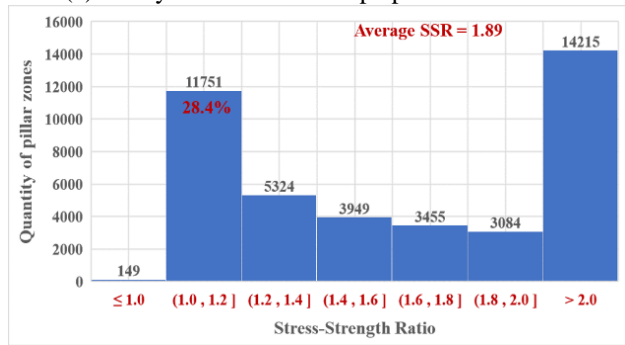
(b)Step 2

Figure 12: Distribution of safety factor

After Step 2, the distribution diagram of stress intensity ratio of stope pillar (Figure. 13) shows that the average safety factor of stope pillar at -210 mL is 1.89, which is higher than that of stope pillar at -150 mL by 1.74. In terms of the number of grid units, the grid units with a safety factor of 1.0~1.2. Stage of -210 mL stope pillar account for 28.4%, while stope pillar at -150 mL is 3.6%. The mining at -210 mL does not affect the safety factor and safety factor distribution of stope pillar at -150 mL. Due to the existence of reserved roof between -150 mL and -210 mL (20 m in thickness), the safety factor of mining pillar at -150 mL does not change with the mining at -210 mL, and the safety factor remains basically unchanged (1.71~1.75).



(a) Safety factor ratio of stope pillar at -150 mL



(b) Safety factor ratio of stope pillar at -210 mL

Figure 13: Stress intensity ratio of stope pillar

4.3 Comparative analysis of variable schemes

Table 3 shows the simulation results of various schemes, including displacement, stope pillar failure unit and safety factor. Through comparative analysis, it can be seen that the mining scheme with 15 m pillar in the stope is better than scheme 1. When the reserved pillar width of the stope is 15 m, stope width (15~18 m) at -210 mL has little impact on the pillar failure unit. The volume of the pillar failure unit changes between 2049.0~2149.4 m³, and the failure ratio changes between 15.9~17.0%, which does not exceed the critical ratio of pillar failure of 19.6%. In scheme 1, the pillar failure in stope is more serious, and the volume of pillar failure unit reaches 2641.8 m³, accounting for 20.9%.

Therefore, from the perspective of the number of pillar failure units in the stope, the mining scheme with 15 m pillar in the stope is better than scheme 1. The mining at -210 mL does not affect the stability of stope pillar at -150 mL, and the tensile and shear failure volume of pillar at -150 mL does not change with the mining at -210 mL, which remains basically unchanged. Due to the existence of reserved roof between -150 mL and -210 mL (20.0 m in thickness), the volume and proportion of failure units of stope pillars left at -150 mL stope will not change with the recovery of -210 mL stopes.

By analyzing the displacement change, plastic zone distribution, principal stress change and safety factor value, it can be seen that schemes 1-4 are in a stable state in the simulation process. Therefore, when scheme 4 is taken as the stope structural parameter at -210 mL, the mine production rate can be maximized.

Table 3: Summary of numerical simulation results of stope stability at -210 mL

Project				1	2	3	4		
				12+12	15+15	16.5+15	18+15		
Displacement (mm)	Step 1	-150 m	Along strike (→)	Max	14.2	14.2	14.2	14.2	
			Gravity direction (↓)	Max	20.2	20.2	20.2	20.2	
	Step 2	-150 m	Along strike (→)	Max	17.9	17.6	17.6	17.5	
			Gravity direction (↓)	Max	39.1	39.7	41.2	42.6	
		-210 m	Along strike (→)	Max	16.3	15.8	15.6	15.4	
			Gravity direction (↓)	Max	20.7	21.5	22.9	24.5	
Failure unit	Step 1	-150 m	Volume /m ³		1879.4	1840.3	1859.1	1871.8	
			Proportion %		19.6	19.2	19.4	19.5	
	Step 2	-150 m	Volume /m ³		1879.4	1840.3	1859.1	1871.8	
			Proportion %		19.6	19.2	19.4	19.5	
		-210 m	Volume /m ³		2641.8	2072.2	2149.4	2049.0	
			Proportion %		20.9	15.9	17.0	16.7	
	Safety factor	Step 1	-150 m	Average safety factor/%		1.71	1.72	1.71	1.72
				<1.2	Proportion	2.7	2.9	2.7	2.5
(1.2, 1.4)				Proportion	59.5	59.7	59.7	60.0	
>=1.4				Proportion	37.8	37.4	37.6	37.5	
Step 2		-150 m	Average safety factor/%		1.73	1.74	1.75	1.74	
			<1.2	Proportion	2.8	3.2	3.2	3.6	
			(1.2, 1.4)	Proportion	58.4	57.7	57.0	56.2	
			>=1.4	Proportion	38.8	39.1	39.8	40.2	
		-210 m	Average safety factor/%		1.74	1.92	1.94	1.89	
			<1.2	Proportion	24.6	16.4	23.2	28.4	
			(1.2, 1.4)	Proportion	26.5	22.2	15.6	12.7	
			>=1.4	Proportion	48.9	61.4	61.2	58.9	

5. Conclusions

- When the roof thickness is 20 m, the ultimate room span calculated by the four theories is safe at 18.8~30.8 m. The room width is proposed as 18 m and the pillar width is 15~18 m from the perspective of safe mining.
- The numerical simulation shows that the two sides of the stope have the maximum horizontal displacement. The roof and floor of the central stope of the panel have the maximum vertical displacement. The failure form of pillars in each stope at -150 mL is mainly tensile failure. The main cause of tensile failure lies in the large deformation of stope roof, floor and two sides. From the point of view of stope stress transfer and release, the local tensile, shear failure and deformation produced by -150 mL will be conducive to the release of stress and the stopes at -210 mL.
- The evaluation of theoretical calculation and numerical simulation shows the optimal stope structural parameters at -210 mL is 18 m in room width, 15 m in pillar width, 60 m in stope length, 40 m in stage height. By optimizing stope structural parameters at -210 mL, equilibrium is realized in production efficiency and ore recovery in open stoping and subsequent backfill of Jama copper mine.

References

- You Xi, Ren Fengyu, He Rongxing, et al. Research In on compressive strength of cemented filling body subsequent filling at the stage of open stope [J]. Journal of Mining & Safety Engineering, 2017, 34 (01): 163-169.
- Liu Guangsheng, Yang Xiaocong, Guo Lijie. Models of three-dimensional arching stress and strength requirement for the backfill in open stoping with subsequent backfill mining [J]. Journal of China Coal Society, 2019, 44 (05): 1391-1403.
- Zhao Kang, Wang Qing, Li Qiang, et al. Optimization calculation of stope structural parameters based on Mathews stabilization graph method [J]. Journal of Vibroengineering, 2019, 21 (4): 1227-1239.
- Long Zhang, Jian-hua Hu, Xue-liang Wang, et al. Optimization of Stope Structural Parameters Based on Mathews Stability Graph Probability Model [J]. Advances in Civil Engineering, 2018, 2018.
- Liu Honglei, Zhao Yong, Zhang Penghai, et al. Stope structure evaluation based on the damage model driven by microseismic data and Mathews stability diagram method in Xiadian Gold Mine [J]. Geomatics, Natural Hazards and Risk, 2021, 12 (1): 1616-1637.
- Sun Mingzhi, Ren Fengyu, Ding Hangxing, et al. Optimization of Stope Structure Parameters Based on the Mined Orebody at the Meishan Iron Mine [J]. Advances in Civil Engineering, 2021, 2021: 8052827.
- Zhang Dongjie, Liu Shuxin, Wang Jianduo. Study on Optimization of Stope Structure Parameters for Steeply Inclined Medium-thick Broken Ore Bodies [J]. Mining, Metallurgy & Exploration, 2022 (prepublish): 1-14.
- Kang Zhao, Qing Wang, Shuijie Gu, et al. Mining Scheme Optimization and Stope Structural Mechanic Characteristics for a Deep and Large Ore Body [J]. JOM, 2019, 71 (11): 4180-4190.
- Pi Kai Zhu, Ji Qing Zhao. Optimization Research of Stope Structural Parameters in Upward Drift Cut-and-Backfill Mining Method [J]. Advanced Materials Research, 2014, 3384: 1010-1012.
- WU Aixiang, HUANG Mingqing, HAN Bin, WANG Yiming, YU Shaofeng, MIAO Xiuxiu. Orthogonal design and numerical simulation of room and pillar configurations in fractured stopes [J]. Journal of Central South University, 2014, 21 (8), 3338-3344.

- [11] Xiang Xing Li, Ke Gang Li. Optimization of Stope Structural Parameters in Phosphorite Mine and its Stability Analysis [J]. Applied Mechanics and Materials, 2014, 3307 (580-583): 1268-1272.
- [12] Tan Yuye, Guo Mochuan, Hao Yimin, et al. Structural Parameter Optimization for Large Spacing Sublevel Caving in Chengchao Iron Mine [J]. Metals, 2021, 11 (10): 1619-1619.
- [13] Lin You. Optimizational Parameters of Stope without Sill Pillar in Metal Mine by Computer Numerical Simulation [J]. Journal of Physics: Conference Series, 2021, 1744 (2): 022095.
- [14] Kengpol, Athakorn, Rontlaong, et al. A Decision Support System for Selection of Solar Power Plant Locations by Applying Fuzzy AHP and TOPSIS: An Empirical Study [J]. Journal of Software Engineering and Applications, 2013,6 (9): 470-481.
- [15] Guo Qi Feng, Ren Fen Hua, Miao Sheng Jun, Chen Xin. Application of Fuzzy Comprehensive Evaluation in Stope Structural Parameters Optimization [J]. Applied Mechanics and Materials, 2012, 256-259 (256-259): 271-275.
- [16] Weidong Song, Dongxu Wang, Yanan Tang. Study on Sublevel Open Stopping with Subsequent Backbackfill Mining Method Stope Parameters Optimization [J]. Advanced Materials Research, 2011, 1270: 250-253.
- [17] Liu P, Zhang. Research on the Optimization of Structural Parameters for Heavy Ore-body by Sublevel Open-Stope with Subsequent Backfill [J]. Metal Mine, China, 2009, 11: 10-13+123.
- [18] T. Malli, M.E. Yetkin, M.K. Özfirat, et al. Numerical analysis of underground space and pillar design in metalliferous mine [J]. Journal of African Earth Sciences, 2017,134: 365-372.
- [19] Terzaghi Karl. Theoretical Soil Mechanics [M]. John Wiley & Sons, Inc. 1943.
- [20] Barton N. Unsupported underground openings [M]. Rock Mechanics Discussion Meeting, BeFo. Swedish Rock Mechanics Research Foundation, Stockholm, 1976.